

Generically, thermoset elastomers are often referred to as rubber. It is characterized by the chemical bonding between polymer chains. One of the important problems that plague elastomer manufacturing and rubber parts under service is cracks. Predicting the main factors affecting crack propagation trajectories during forming and after curing time is an important challenge. For this purpose, numerical analysis was implemented by using the commercial ABAQUS/CAE software package. A three-dimensional model was established to predict the important factors that affect this process. During the analysis, the effect of forming velocity and the amount of kinetic energy on the distortion of rubber material and crack propagation is explored in detail by using different forming punch velocities. The drop velocity of the upper insert (punch) on the rubber pad was taken as 10 m/s, 7 m/s, and 5 m/s, respectively. Consequently, while each forming velocity will generate different kinetic energy between the interaction surfaces, the change in crack behavior and the normal stress can be monitored in different positions. As a result, among these velocities, it was found that the low forming velocity of the upper insert (punch) is better than the others in forming rubber where cracks and distortions were at minimum values. Also, the amount of kinetic energy is low enough in the case of low speeds and can affect the results significantly. In addition, it was found that the generated stresses have a significant impact on the crack development in a specific area, especially near the fillets and sharp edges. It was concluded that calculating the parameters affecting the crack growth and predicting the crack propagation trajectories using the finite element method is a significant method for predicting and solving crack problems before tool fabrication

Keywords: rubber crack, rubber pad, numerical analysis, elastomer forming, crack propagation, ABAQUS

NUMERICAL SOLUTIONS FOR CRACK PROBLEMS DURING ELASTOMER FORMING

Badr Kamoon

Corresponding author

Department of Machinery and Equipment Engineering
Technical College Al-Mussaib*

E-mail: com.bdr@atu.edu.iq

Salam O. Dahi

Department of Machinery and Equipment Engineering
Technical College Al-Mussaib*

Hamzah Kadhim

Department of Mechanical
Karbala Technical Institute*

*Al-Furat Al-Awsat Technical University
Imam Ali Bridge, Najaf, Iraq, 54003

Received date 09.09.2022

Accepted date 28.11.2022

Published date 30.12.2022

How to Cite: Kamoon, B., O. Dahi, S., Kadhim, H. (2022). Numerical solutions for crack problems during elastomer forming. *Eastern-European Journal of Enterprise Technologies*, 6 (1 (120)), 83–90. doi: <https://doi.org/10.15587/1729-4061.2022.268285>

1. Introduction

Cracking in parts under service is a great challenge in the industrial field due to the main impact of crack behavior on part performance. Cracks start normally with micro-cracks and develop with elevated working temperature, load change, and other factors. Many researchers spot the light on the mechanism of crack initiation and development following different methods and analyses.

Some studies used a traditional fatigue method to deal with this type of problem, and others adopted fracture mechanism theories to estimate and forecast the trajectories of crack growth rate. According to much literature and engineering database in this field, the parameters related to crack behavior at different steps such as preparation, manufacturing, and working conditions were determined based on the infield engineering data.

Consequently, these studies almost depend on the experience that performs poorly and only provides rough solutions, while estimation according to accurate analysis and up-to-date calculation by numerical investigation are better. Since the elastomer industry is developing rapidly, numerical analysis is becoming the best solution to predict and determine crack problems before the component failed.

Therefore, research on the development of this direction is concentrated on the problem under the current study to determine better visualization and recommendations. The behavior of elastomer material during forming varies according to many factors such as shape geometry, physical properties, and loading conditions. This variation is difficult to predict due to the nonlinearity behavior of this material. Consequently, building new knowledge and a clear vision by adopting the numerical technique will lead to minimizing this problem and prevent product failure.

2. Literature review and problem statement

Rubber parts are used in many industrial applications such as automobiles, hydrants, gaskets valves, and fittings. The major service problems of elastomers are that they are quickly degraded more than expected creating many difficulties for utilities to cost and programs to plan preventive maintenance. Elastomers are normally characterized by their low tensile strength (1–10 MPa), high extensibility, and electrical insulation. Thermoset elastomers can be highly affected by weak stress and return to their original shape after the stress is removed. The problem of estimating the imposed

strain that leads to cracks propagating under different temperatures was investigated. However, the effects of strain rate on the value of the critical length during crack propagation still need to be solved [1, 2].

In [3, 4], the elastomer membrane under tension and the propagation of dynamic cracks in elastomer parts, and the crack speed measured along the crack zone were investigated analytically. The methods involve stretching an elastomer part and then initiating a small crack. It was found that the crack propagation zone follows the stretch direction of the crack. This method is limited to the analysis of cracks with constant crack speed and direction.

The works [5, 6] show that the most popular approach to simulate the cracks' behavior during their life cycle is the finite element method. Many finite element codes can describe the hyperplastic behavior of rubber as a nonlinear elasticity behavior. Large deformations and large displacements occur during the forming process. By using finite element software, the growth and behavior of cracks can be estimated with less time and minimum cost. Graphical demonstrations and numerical computations are always used successfully to observe the effect of the geometry conditions, elastic constants ratio, and stresses on the stress intensity factors at the crack tips. The approach here is used for the two-dimensional crack problems and cannot be extended to three-dimensional ones due to geometry constraint problems.

In [7], LS-DYNA finite element software is used for modeling and simulating a rubber pad in the stamping process. The forming parameters such as rubber pad hardness, model, and friction coefficient of the blanks were successfully determined, and the result was 50 % CPU time-saving. However, some problems in this method are linked to the appearance of negative volume due to the formation of small-size elements.

In [8], simulations and experiments were carried out by using a family group of a matrix of the polydimethylsiloxane (PDMS) embedded elastomer with two spherical glass beads. The aim is to generate high triaxial stress. The result shows that the increase in loading will lead to an increase in stress on the deformed surface and cracks may spread out to critical points. Also, the micro-crack may grow and transit at some critical points.

In [9], ABAQUS/Standard finite-element code is used to analyze and simulate semi-elliptical surface cracks for composite aluminum plates. The uniaxial tensile load was applied on the repaired cracked plate to evaluate the failure strength and stress intensity factors (SIF). The results show that the stress concentration depends on both the patch thickness and crack depth. However, increasing layer thickness will increase the possibility of surface cracks with depths greater than expected.

In [10], a nonlinear finite element analysis is used to model and analyze dynamic crack propagation in rubber. As a result, the influence of some parameters such as surface energy, viscoelastic dissipation, and inertia effects has been investigated. The fracture energy in the vicinity and surrounding of the crack tip is a problem to be solved.

The papers [11, 12] show that by identifying the problems of potential forming, it is possible to reduce the time, cost, and cycle of product development by using numerical simulation (ABAQUS). Also, the part quality can be improved during manufacturing to ensure appropriate processes.

The paper [13] approved that the viscoelastic modulus highly affects crack propagation in rubber. The nucleation of cracks is stress-aided, so the crack nucleation rate will increase if the viscoelastic loss peak is shifted. It was found

that rubber materials have a larger crack propagation energy when the viscoelastic peak is low.

The method in [14] attempts to provide a suitable prediction of the tearing energy by calculating the dissipated energy due to different inelastic processes. The results show that the classical method overestimates the critical tearing energy by approximately 15 %.

It was found that the crack propagation energy in front of viscoelastic deformations of rubber and the role of this propagation for sliding friction with rolling resistance and rubber typically depend on the nature of the surface itself [15, 16].

The above sources deal with many cases of crack propagation trajectories, and each one has dealt with different aspects. The majority of these sources are involved with crack development under different loading and working conditions. It will be more valuable to explore other important effects such as the effects of forming velocity and kinetic energy on the crack trajectories. The current research aimed to describe the cracks' behaviors under different forming velocities. The effects of speed change between the contact surfaces and layer thickness on crack development were investigated. The ABAQUS/CAE finite element software was adopted to simulate the growth of these cracks at different punch-forming velocities. Some sidewall cracking may be linked to the generation of stress during rubber shrinkage and early thermal contraction. These problems may cause a rapid increase in crack propagation and need to be solved. The intensity of stresses and strains was investigated to describe the crack extension while working.

3. The aim and objectives of the study

The aim of the current study is to identify regularities of the crack development trajectories during elastomers forming by using a numerical analysis method.

The objectives below have been adopted to achieve the aim:

- to predict the crack's trajectories under different forming velocities, and explore the kinetic energy required for this process by developing a finite element model;
- to estimate the cause of stresses affecting the mechanical behavior of the rubber bushing subject during the forming process.

4. Materials and methods

4.1. Part geometry and material properties

In this research, rubber bushing geometry is built by CAD (3-D) using the CATIA V5 design program in order to process and develop the finite element model. Fig. 1, 2 illustrate the geometry of a rubber pad used for the analysis process in 2-D and 3-D, respectively.

The rubber type used in this research is MAT27, and the main mechanical properties of this type of rubber are listed in Table 1. Shore units are normally used in measuring rubber hardness.

Mathematically, the strain energy density (ϵ) during rubber forming can be defined by the following equations:

$$\epsilon = A(K_1 - 3) + B(K_2 - 3) + C(K_3^2 - 1) + D(K_3 - 1)^2, \quad (1)$$

where $C = 0.5A + B$, K_1 , K_2 , K_3 is an invariant of right Cauchy Tensor C ;

$$D=A(5v-2)+B(K_2v-5)/2(1-2v), \tag{2}$$

where v is Poisson's ratio.

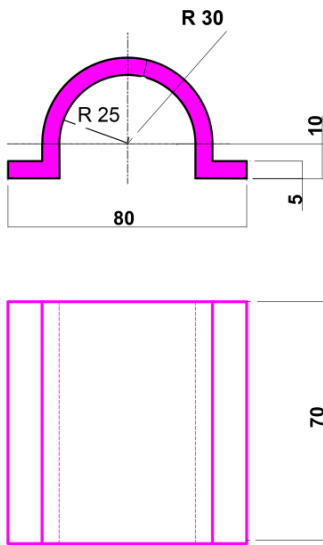


Fig. 1. The rubber product including all dimensions

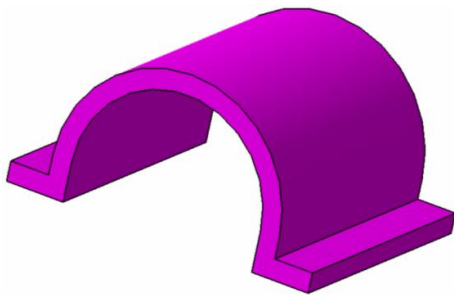


Fig. 2. Product under analysis in three dimensions

Table 1

Mechanical properties of rubber

No.	Type	A	B	Density (kg/m ³)	Poisson's Ratio
1	Shore 90	2.8	0.71	1.1×10 ⁻⁹	0.5

The steel type used for forming parts (punch and die) is tool steel with a Young's modulus of elasticity 206 GPa and 0.3 Poisson's ratio.

The tooling for this manufacturing process encompasses many important parts. The main parts are the upper core (punch) and lower insert (die).

To avoid and prevent any interference between the parts during forming, and to decrease the error and time during the simulation, all these mold parts and assembly will be modeled according to their actual dimensions and tolerances. This modeling will support a better understanding of building the simulation process according to actual conditions and enhance the final results. The CATIA V5 R16 software is adopted for modeling this process.

The procedure of forming the rubber sheet includes three sequence steps. These steps involve aligning the rubber material between the punch and die, moving the punch down the blank to press the material inside the die cavity, and finally ejecting the product. These steps are illustrated in Fig. 3, 4 below.

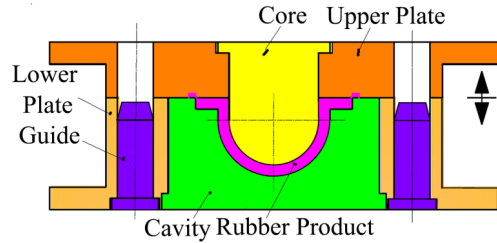


Fig. 3. Mold assembly parts during forming

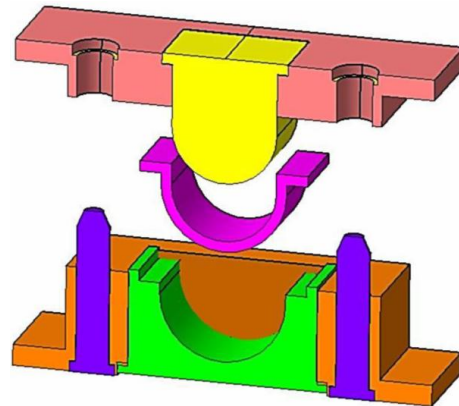


Fig. 4. Cross-section of the assembly tools during the part ejection

For accurate results, only the interaction parts (upper insert, lower insert, and rubber material) will be simulated in the assembly.

4. 2. Finite Element Process

In this work, the numerical analyses were performed by using commercial FEM software (ABAQUS/CAE) to establish analysis and simulation of this model. The parts are modeled by using CATIA V5, and then exported to ABAQUS/CAE for the simulation process. The completed procedure and steps of analysis are shown by the flowchart in Fig. 5.

The forming process of the rubber part starts with filling the upper insert cavity with the rubber blanks material. This rubber consists of some components such as base rubber, curing agent, and filler like carbon black. Also, some components may be added like adhesion agents, chemical additives, and antioxidants.

Making a contact between rubbers and insert surfaces is the initial step in the simulation process. The gap between the upper and lower inserts represents the product thickness. The contact step between the surfaces is illustrated in Fig. 6.

During forming, the rubber folds will be distributed in the gap between the upper and lower inserts to form the final product shape.

Based on elastic layered system theory, the boundary conditions involve a full constraint of the lower insert to prevent it from any motion in any direction. The boundary conditions were set as no rotation and no displacement at some other supporting parts. Also, a uniform pressure of 1000 MPa will be applied to the upper insert. Fig. 7 shows the boundary conditions and applied pressure.

In terms of parts deformation, the rubber sheet is classified as a deformable part, while the upper and lower inserts are classified as a rigid body. The relationship between the rigid body and the deformable part is represented as master and slave.

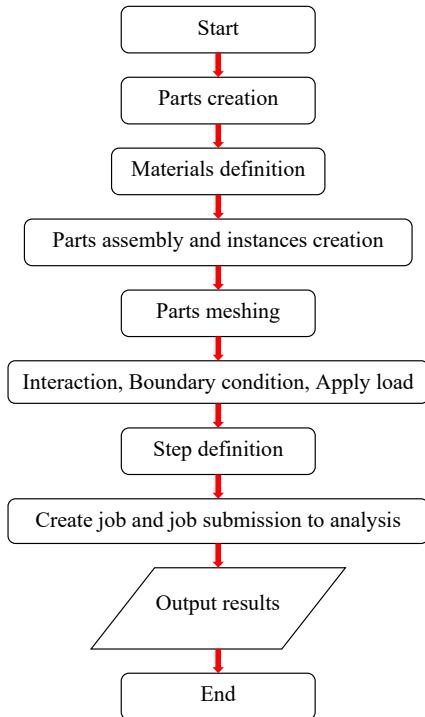


Fig. 5. Flowchart of the completed procedure and steps of analysis

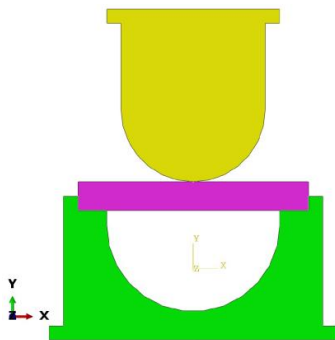


Fig. 6. Contact behavior between surfaces before forming

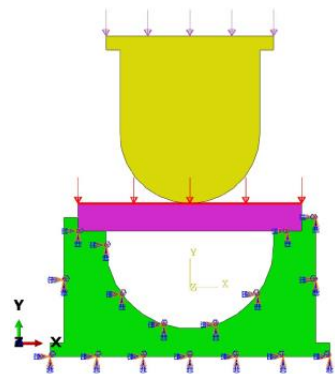


Fig. 7. The boundary conditions and applied pressure representation

The upper part will move downward to be in contact with the rubber and stop after the part forming process is completed. The upper part will move up toward the cavity and press the material to the desired shapes before stopping.

Rubber is a very soft material and considered a deformable material (fully hyperelastic) with a high strain level so

it is modeled as a hyperelastic model, which is defined as a strain energy function. As a large strain occurs, the tetrahedral mesh type is used for meshing the rubber parts.

Other parts are meshed by hexahedral mesh type to yield reasonable results. The finite element mesh of the parts is shown in Fig. 8.

Calculating the number and position of elements is an important step that allows estimating the values of strain and stress at each element and leads to accurate results. Labeling all the important elements will enable us to extract accurate results. In this model, the total elements of the whole model are 17,676 elements.

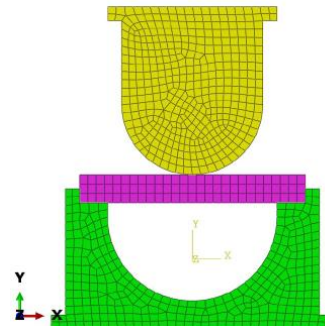


Fig. 8. Parts mesh and elements labeling representation

In Fig. 8 E-model, the hyperelastic rubber component is modeled using the CAX4H element used in the analysis of this model, and the mesh size of this highly non-linear rubber component model is between 1.4 mm to 1.6 mm. These types of elements are suitable for simplifying the boundary conditions and loading.

Determination of the number and position of elements is an important step that allows estimating the values of strain and stress at each element and leads to accurate results. In this model, the total elements of the whole model are 17,676 elements.

The FRICTION, ROUGH option is normally used in ABAQUS to represent the frictional behavior as sticking friction. During contact and interference between rigid bodies (masters) and deformable parts (slaves), the assumption was that the rigid body has a lubricated surface and the friction coefficient between them is a small value (0.05).

Rubber behavior during forming is classified as non-linear elastic. Rubber folds will be distributed under the applied pressure to the vicinity cavity, which equals product thickness. The cavity gap between the upper and lower inserts will be filled with rubber to form the final product.

The nonlinearity behavior of rubber is a function of strain energy and is referred to the properties of this material as an elastic material.

5. Results of numerical analysis during elastomer forming

5.1. Results of rubber formation under different forming velocities

A feasible model was established, and the ABAQUS finite element software was used for numerical analysis. In the current work, the aim is to analyze the impact of deformations on the initiation of crack development in rubber material. During fracture initiation, critical tension occurs driven by the strain softening. Failure and crack description in simu-

lations that were plugged by ABAQUS was performed using fine meshes to investigate the influences.

With ABAQUS/CAE, the forming process is simulated in two steps. The high values of strain generated due to the applied pressure will decrease or be prevented by increasing the contact zones between the insert surfaces and the rubber pad. At the start of the forming process, the strain will reach its peak values due to the movement of the highly energized particles and highly dislocation forces, especially between the contact forming surfaces.

The shear stress, normal stress, and stress intensity of the crack tip under different loading conditions were estimated. Also, at the crack tip, the shear stress and principal stress intensity can reflect the cracking situation. In the first step of the analysis, the upper insert force is applied. The punch (rigid body) is moved down 70 mm in the second step of the analysis, and the peak velocity occurs in the middle of the time period. Because the fundamental mode of vibration is low, and the rubber blank is very flexible, the simulation would take more time to obtain the analysis results. Different forming velocities were used as 10 m/s, 7 m/s, and 5 m/s, respectively. When the punch drops from the hydraulic press with a velocity of 10 m/s, it was found that the distortion zone of rubber is too large, with many visible cracks in the adjacent zones (red zones). This can be attributed to the high amount of kinetic energy applied to the model. This case is illustrated in Fig. 9 below.

The kinetic energy in rubber elements during folding for the above step is too high as shown by the energy-time plot in Fig. 10.

Based on the above results, the punch drop velocity should be less valued and taken to be 7 m/s. However, the distortion occurred but the folding of rubber layers is less than the previous one. In addition, it can be seen that there are fewer cracks in adjacent zones than expected (fewer red color zones). The contour plot in Fig. 11 shows that the rubber product started to relax from distortion and changed to green color, and only a small zone is affected by distortion with minimum cracks.

In this forming step, the amount of kinetic energy in rubber elements will be less than in the previous step as shown by the energy-time plot in Fig. 12.

In the third and last forming step using a punch drop velocity of 5 m/s, the rubber layers are folded smoothly, and the amount of kinetic energy is less than in the previous steps. The product is expected completed uniformly without distortion and cracks. This forming step is illustrated by the contour plot in Fig. 13.

Fig. 14 shows that a minimum of kinetic energy is consumed at this forming speed.

The results above reveal the important effect of the forming speed on cracks and non-uniform distortion generated in rubber products. Choosing the optimum forming

speed will allow facilitating the process and obtaining a highly accurate product.

The high strain values generated due to the high kinetic energy will increase the contact zones between the insert surfaces and the rubber pad. At the start of the forming process, the strain will reach its peak values due to the movement of the highly energized particles and highly dislocation forces, especially between the contact forming surfaces.

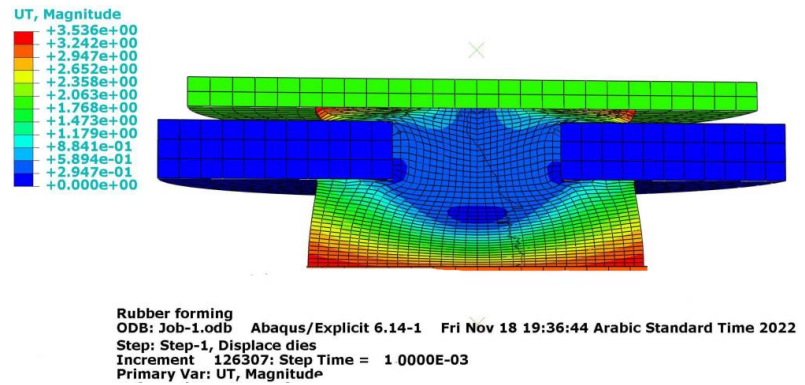


Fig. 9. The contour plot of forming the rubber pad at high punch drop

Printed using Abaqus/CAE on: Fri Nov 18 20:57:22 Arabic Standard Time 2022

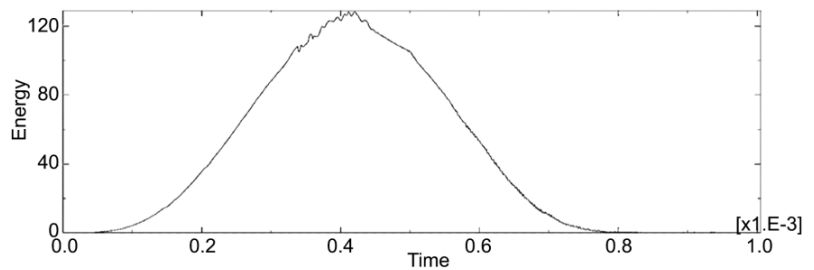


Fig. 10. Energy-time plot during the first step

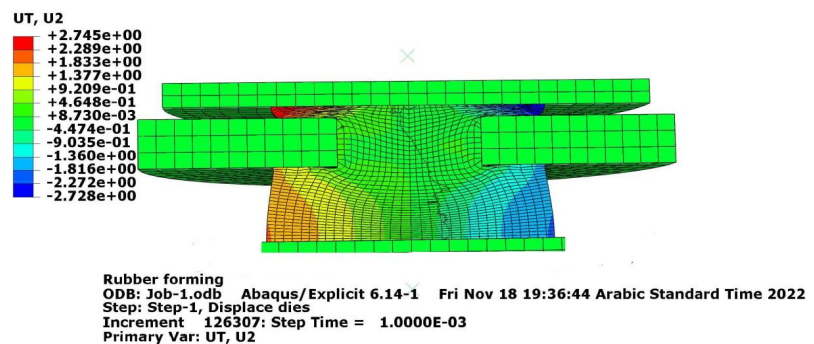


Fig. 11. The contour plot of the forming at high punch drop

Printed using Abaqus/CAE on: Fri Nov 18 20:56:11 Arabic Standard Time 2022 [x1.E3]

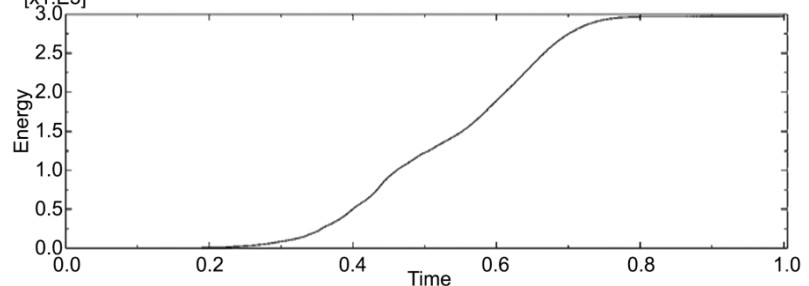


Fig. 12. Energy-time plot at 7 m/s punch speed

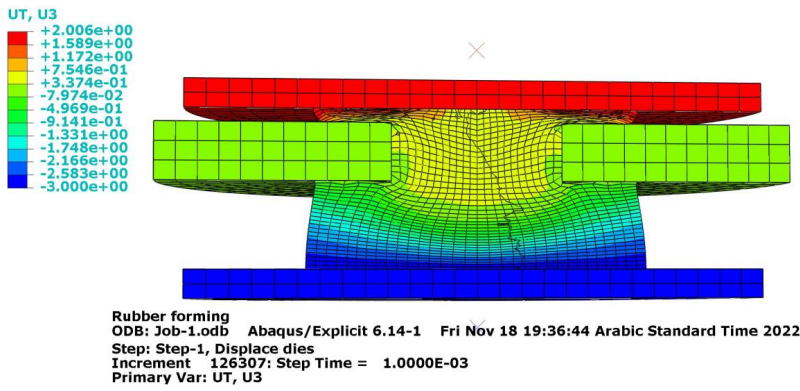


Fig. 13. The contour plot of the last forming at 5 m/s punch drop

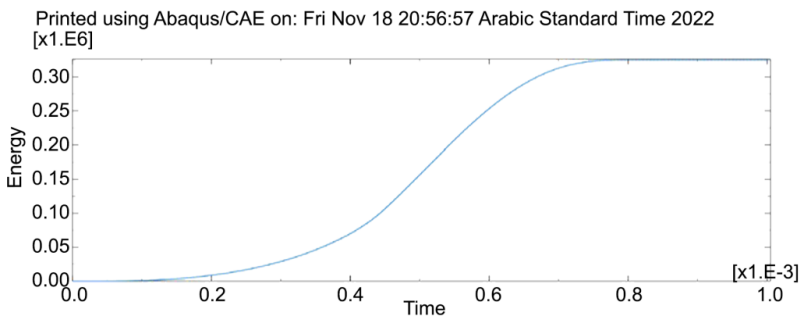


Fig. 14. Energy-time plot at 5 m/s punch speed

5. 2. Results of stress generation and mechanical behavior of rubber bushing during forming

The distortion and contact instabilities will take place during the rubber pad forming due to large strain occurring in the simulation process.

The shear stress, normal stress, and stress intensity of the crack tip under different loading conditions were estimated. Also, at the crack tip, the shear stress and principal stress intensity can reflect the cracking situation. The contours of axial stresses of the deformed mesh show that the maximum stresses will occur in the sharp and the fillet zones (radius) and along the parting line between the upper and lower inserts. The generation of stresses during the forming process is illustrated by the contour graph in Fig. 15.

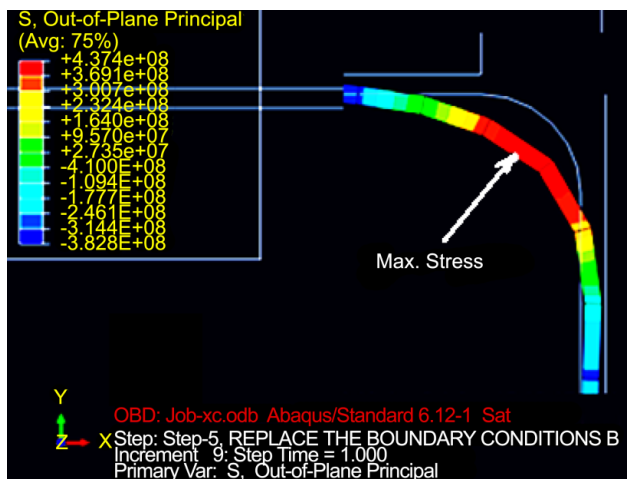


Fig. 15. Contour graph of generated stress during the forming process

The pressure adjustment and calibration during action onto the rubbers will prevent high strains by increasing the contact area between the blanks and inserts. Large deformations can be undergone by softer materials and lead to generating high strain-stress concentrations. Material orientation and distribution during the final step of simulation in the forming process under some variables like pressure and temperature are like different surfaces meeting together to contact with each other and generating a single surface.

The imposed constraints on the part thickness will build connecting elements and nodes along the fillet radius and surface curvature according to the shape topology to form the final thickness, as shown in Fig. 16.

In the numerical model, the position of the crack threshold was obtained and evaluated. Crack propagating near the fillet zones (R) and the sharp edge is developing steadily due to non-uniform stretch forming in this area and this causes high stress concentrations.

Larger strains will occur during the crack. This strain concentration is important because the material structure will evolve with strain development. It is possible to model the nonlinearities of the physical model as boundary nonlinearities like friction and contact, material nonlinearity, and large displacement effects.

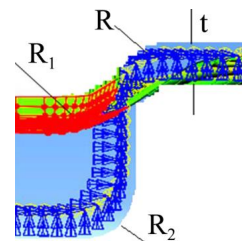


Fig. 16. Elements and nodes topology along the fillet and surface curvature

After upsetting the product, the curing starts and the part begins to shrink to the actual dimensions. However, the shrinkage in the small value dimension is not visible, especially at the wall thickness. Sometimes, and due to many reasons such as non-homogenous pressure distribution, the thickness in fillets and corners will be greater than in other zones. This will lead to an increase in the thermal stresses due to high-temperature concentration in these zones. The dimension stability is one of the major problems in forming a hyperelastic material.

One of the most possible solutions for this problem is to add some additives such as fillers or fiber to increase the binding forces between material crystals.

6. Discussion of the analysis results of forming the elastomer pad

The finite element can mimic the general behavior of the rubber pad very well during different punch velocity drop and loading steps. It is considered a better choice to model hyperelastic materials like rubber. The behavior of rubber

material is always time-dependent, and the strain rate has the main impact on the stiffness increase in rubber forming.

In some particular areas, the mechanical response of the stress intensity is normally a high-order polynomial, and due to large deformations, high stress strains at the crack zone can be absorbed by soft materials as explained in Fig. 15.

The rate of crack propagation has a comprehensive effect and characterization on the local morphology of the part. Cracks will follow different paths and develop in many directions such as vertical or horizontal. The value of stress at a circular crack strongly depends on crack sharpness, which affects the material failure as mentioned in Fig. 16.

Distortion and contact instabilities will take place during the rubber pad forming due to large strain occurring in the simulation process. The movement and dislocation of rubber elements will generate kinetic energy according to the impact between the interaction surfaces (Fig. 10, 12, 14). Numerical mass damping is used to prevent some oscillations that happened during the first interaction between the rubber and other parts, and the hourglass mode is always used to prevent this problem.

In the other simulated tests, there is considerable deformation in many layers. It is possible to explore that the rubber material is deformed very fast in the pressure direction. The forming rubber appears to be stuck to the inner surface of the cavity due to the friction force. In the last simulation step, the deformed rubber will contact all cavity surfaces to fill the 5 mm thickness between the upper and lower inserts. During forming, the relative movement between the rubber and upper insert leads to the distribution of the molten uniformly inside the cavity. During impact, the rubber elements distort too much and penetrate the elements. To minimize these influences, which affect the system stability, the pressure should not exceed 0.95 MPa.

As a comparison with the finding of other researchers in the same field, the finding of the current work is nearly close to the work [1]. It was found that the crack propagation behavior in rubber materials due to high stresses causes the rubber to lose some of its elasticity and allows surface cracks to appear eventually. Some limitations were recorded in this study, and this is normally related to the hyperelasticity behavior of this material. The nature of element type randomly deforms under some boundary conditions. In this case, the thickness may vary in some zones. The disadvantage in dealing with this analysis method normally requires a long time of simulation running to find accurate results. Consequently, determining the suitable boundary conditions and interaction types between the contact parts will significantly enhance the results.

7. Conclusions

1. The analysis and evaluation of the rubber-forming process through different steps were carried out according to the relevant geometrical properties of the specific component.

During simulation, the crack's trajectories under different punch-forming velocities are investigated.

During these sequence steps, the interaction between the parts according to the rule of master (non-deformable part) and slave (deformable part) will make the rubber deform to fill the cavity space according to the forming speed. The high forming speed will result in a nonhomogeneous layer distribution, and the random movements of nodes and elements will cause a successive dislocation between the layer's boundaries. In this case, and due to high particle movements, the crystals will collide with each other and gain high energy leading to high distortion and non-uniform forming. The effects of a random increase in the forming speed and load on crack propagation are largely due to the increase in kinetic energy, and this will increase the possibility of crack initiation by more than 15 %.

The low-speed forming will lead to smooth folding of the rubber layers with less generated energy, and the possibility of crack generation will decrease.

2. The mechanical behavior of rubber material during forming is a complex process. During punch drop, the elements near the fillets and sharp zones may be suffering from the lack of enough compression and filling according to the forming speed. This leads to making these areas weak and highly stressed zone, and the possibility of crack initiation is 25 % higher than in the case of uniform pressure distribution. These non-uniform dislocations are considered the main reason for forming some weak points that develop and spread out with time to initiate a crack. Also, it is a high impact on the mechanical properties of the final product. The load should be distributed uniformly to prevent cracks due to the high impact of non-uniform pressure distribution on crack initiation and development.

Finally, developing a finite element model is a suitable way of understanding the behavior and mechanism of elastomer forming. This will help the manufacturer to evaluate problem conditions more comprehensively and make true decisions in design before tooling investment.

Conflict of interest

The authors declare that they have no conflict of interest in relation to this research, whether financial, personal, authorship or otherwise, that could affect the research and its results presented in this paper.

Financing

The study was performed without financial support.

Data availability

The manuscript has no associated data.

References

- Scetta, G. (2020). Fatigue cracking of thermoplastic elastomers. Université Paris sciences et lettres. Available at: <https://pastel.archives-ouvertes.fr/tel-03149063>
- Samarth, N. B., Mahanwar, P. A. (2021). Degradation of Polymer & Elastomer Exposed to Chlorinated Water – A Review. *Open Journal of Organic Polymer Materials*, 11 (01), 1–50. doi: <https://doi.org/10.4236/ojopm.2021.111001>

3. Corre, T., Coret, M., Verron, E., Leblé, B. (2021). Non steady-state intersonic cracks in elastomer membranes under large static strain. *Journal of Theoretical, Computational and Applied Mechanics*. doi: <https://doi.org/10.46298/jtcam.6906>
4. Poulain, X., Lefèvre, V., Lopez-Pamies, O., Ravi-Chandar, K. (2017). Damage in elastomers: nucleation and growth of cavities, micro-cracks, and macro-cracks. *International Journal of Fracture*, 205 (1), 1–21. doi: <https://doi.org/10.1007/s10704-016-0176-9>
5. Wang, H., Wu, Y., Yang, J., Wang, H. (2021). Numerical Simulation on Reflective Cracking Behavior of Asphalt Pavement. *Applied Sciences*, 11 (17), 7990. doi: <https://doi.org/10.3390/app11177990>
6. Hamzah, K. B., Nik Long, N. M. A., Senu, N., Eshkuvatov, Z. K. (2021). Numerical Solution for Crack Phenomenon in Dissimilar Materials under Various Mechanical Loadings. *Symmetry*, 13 (2), 235. doi: <https://doi.org/10.3390/sym13020235> Halkacı, H. S., Öztürk, E., Türköz, M., Dilmeç, M. (2017). 2D Finite Element Analysis of Rubber Pad Forming Process. 2nd International Conference on Science, Ecology and Technology-2016 (ICONSETE'2016). Available at: <https://www.researchgate.net/publication/312198030>
7. Oscar, J., Centeno, G. (2017). Finite Element Modeling Of Rubber Bushing For Crash Simulation Experimental Tests and Validation. Division of Structural Mechanics, Lund University. Available at: <https://www.byggmek.lth.se/fileadmin/byggnadsmekanik/publications/tvsm5000/web5163.pdf>
8. Iváñez, I., Braun, M. (2017). Numerical analysis of surface cracks repaired with single and double patches of composites. *Journal of Composite Materials*, 52 (8), 1113–1120. doi: <https://doi.org/10.1177/0021998317722044>
9. Elmukashfi, E., Kroon, M. (2020). Numerical Modeling and Analysis of Dynamic Crack Propagation in Rubber. 13th International Conference on Fracture. Beijing. Available at: <https://www.researchgate.net/publication/346898728>
10. Magid, H. M., Dabis, B. K., Abed alabas Siba, M. (2021). Analysis of the main factors affecting mass production in the plastic molding process by using the finite element method. *Eastern-European Journal of Enterprise Technologies*, 6 (1 (114)), 65–71. doi: <https://doi.org/10.15587/1729-4061.2021.248375>
11. Kadhim, K. J., Jaber, J. A., Ibrihim, H. R. (2022). Implementation of finite element analysis for solving the constraints in forming process of large steel parts. *Eastern-European Journal of Enterprise Technologies*, 4 (1 (118)), 64–71. doi: <https://doi.org/10.15587/1729-4061.2022.263452>
12. Persson, B. N. J., Albohr, O., Heinrich, G., Ueba, H. (2005). Crack propagation in rubber-like materials. *Journal of Physics: Condensed Matter*, 17 (44), R1071–R1142. doi: <https://doi.org/10.1088/0953-8984/17/44/r01>
13. Elmukashfi, E. (2015). Modeling of fracture and damage in rubber under dynamic and quasi-static conditions. School of Engineering Sciences, Department of Solid Mechanics, Royal Institute of Technology. Stockholm. Available at: <http://kth.diva-portal.org/smash/get/diva2:876354/FULLTEXT01.pdf>
14. Maiorova, K., Vorobiov, I., Andrieiev, O., Lupkin, B., Sikulskiy, V. (2022). Forming the geometric accuracy and roughness of holes when drilling aircraft structures made from polymeric composite materials. *Eastern-European Journal of Enterprise Technologies*, 2 (1 (116)), 71–80. doi: <https://doi.org/10.15587/1729-4061.2022.254555>
15. Korzhyk, V., Khaskin, V., Grynyuk, A., Peleshenko, S., Kvasnytskyi, V., Fialko, N. et al. (2022). Comparison of the features of the formation of joints of aluminum alloy 7075 (Al-Zn-Mg-Cu) by laser, microplasma, and laser-microplasma welding. *Eastern-European Journal of Enterprise Technologies*, 1 (12 (115)), 38–47. doi: <https://doi.org/10.15587/1729-4061.2022.253378>